Letters

Dual Receiver Coils Wireless Power Transfer System With Interleaving Switching

Kye-Seok Yoon, *Student Member, IEEE*, Sang-Han Lee, In-Kui Cho, Ho-Jin Lee, and Gyu-Hyeong Cho, *Fellow, IEEE*

***Abstract*—This letter presents a wireless power transfer (WPT) system for wristband device charging. By using dual receiver coils with power switches in an interleaved manner, the proposed WPT system can simultaneously operate to accumulate energy from the primary coil and transfer the previously accumulated energy to the battery in each coil. As a result, the WPT efficiency can be increased with the small coils, even at high load resistance. The proposed WPT system is theoretically analyzed by a lumped circuit model and verified by measurement using prototype boards. Compared with the conventional WPT structure that uses one receiver coil (2 cm × 5 cm), the proposed WPT system with two receiver coils (each 2 cm × 2.5 cm) achieved a 6.67% end-to-end power efficiency improvement at the output resistance of 100 Ω under the same condition of the coil dimension and the resonant frequency of 140 kHz.**

***Index Terms*—Dual receiver coils, high efficiency, wireless power transfer (WPT), wristband wearable device.**

I. Introduction

WRISTBAND wearable devices have been widely used to continuously monitor the vital signals for various purposes, such as traffic safety, health care, and medical research [1]–[3]. For the daily usage of the devices, the intermitted charge of rechargeable batteries is required, which reduces the convenient use. To improve usability, wireless power transfer (WPT) systems for the wrist devices have been studied [4]–[7]. Generally, a simple configuration of a two-coil WPT system, which is largely divided into a transmitter (TX) and a receiver (RX), has been adopted, as shown in Fig. 1. The TX consists of an inverter, a TX matching capacitor, and a primary coil. The RX is composed of a secondary coil, an RX matching capacitor, a rectifier, a dc–dc converter, and a battery. To analyze it from a circuit perspective, this structure can be modeled as the equivalent lumped elements, as shown in Fig. 2(a) [8], [9], [18]–[21]. For TX, the inverter can be modeled as voltage source (V_s) in series with inductance of the primary ($L_{\rm TX}$), capacitance of the TX ($C_{\rm TX}$), and the parasitic resistance ($R_{\rm TX}$) that is the sum of a TX ESR coil resistance with a TX electronic device resistance. Likewise, the RX parts of electronic devices can be modeled as a load resistance (R_L) in series with inductance of the secondary ($L_{\rm RX}$), capacitance of the RX ($C_{\rm RX}$), and the parasitic resistance ($R_{\rm RX}$) that is the sum of an RX ESR coil resistance with an RX electronic device resistance. For an intuitive analysis, the effect of RX is abstracted as a reflected resistance $R_{\rm refl}$ at the resonant frequency, as shown in Fig. 2(b) [10]. $R_{\rm refl}$ is not real resistance but symbolic resistance, in which the power dissipation is equivalent to the actual power transferred to RX, and can be defined as follows:

$$R_{\rm refl} = \frac{M^2 \cdot w^2}{R_{\rm RX} + R_L} \tag{1}$$

where M and w are the mutual inductance and the angular frequency, respectively. Therefore, total efficiency of WPT ($\eta_{\rm total}$)

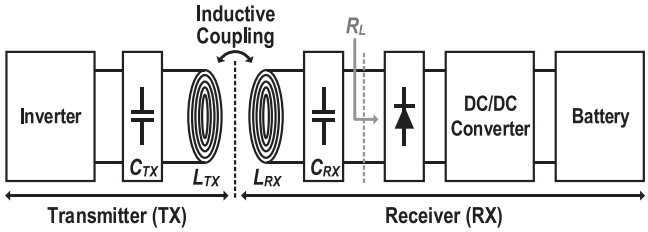

Fig. 1. Conventional configuration of a two-coil wireless power transfer system.

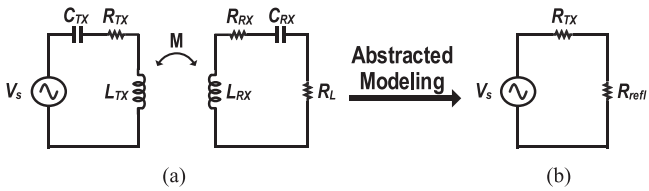

Fig. 2. (a) Equivalent lumped elements of a two-coil wireless power transfer system. (b) Abstracted modeling of the effect of RX at the resonant frequency.

Manuscript received January 16, 2018; revised March 4, 2018; accepted March 23, 2018. Date of publication April 5, 2018; date of current version September 28, 2018. This work was supported by a National Research Council of Science and Technology grant by the Korea Government [18ZR1240, Development of core technology for middle-range wireless power transfer technology]. *(Corresponding author: In-Kui Cho.)*

K.-S. Yoon, S.-H. Lee, and G.-H. Cho are with the School of Electrical Engineering, Korea Advanced Institute of Science and Technology, Daejeon 34141, South Korea (e-mail:

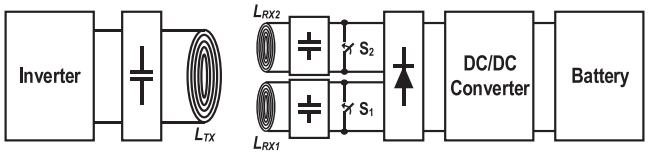

Fig. 3. Proposed wireless power transfer system.

can be defined as follows [11]:

$$\eta_{\text{total}} = \eta_{1,2} \cdot \eta_{2,L} = \frac{R_{\text{refl}}}{R_{\text{TX}} + R_{\text{refl}}} \cdot \frac{R_L}{R_{\text{RX}} + R_L} \tag{2}$$

where $\eta_{1,2}$ and $\eta_{2,L}$ are the power efficiency delivered from the TX to the secondary coil and that delivered from the secondary coil to the R_L, respectively. According to (2), the tradeoff relationship between $\eta_{1,2}$ and $\eta_{2,L}$ depends on R_L: in the case of high R_L, $\eta_{1,2}$ is low but $\eta_{2,L}$ is high. Otherwise, $\eta_{1,2}$ is high but $\eta_{2,L}$ is low. In the WPT system for a wearable device, it is hard to achieve high $\eta_{1,2}$, because the sizes of the battery are limited. In case of small battery, the maximum charging current is considerably limited to make the battery life last longer [12], and its low charging current is equivalent to a high R_L. In addition, the size of the RX coil is also limited to that of the wearable device, which leads to low *M* that is related to the size of the RX coil. As a result, the WPT efficiency of portable device charging is limited by both high R_L and low *M*, when the conventional structure is used [13]–[15].

To solve this issue, a dual RX coils WPT system for wristband device charging is proposed. By using dual coils of RX in an interleaved manner, the WPT efficiency can be increased with the small coils, even at high R_L. The paper is organized as follows. In Section II, the concept of the proposed WPT system is explained and analyzed. Measurement results and performance comparison are presented in Section III; a brief conclusion is provided in Section IV.

II. Proposed Wireless Power Transfer System

The configuration of the proposed WPT system is the same as that of the conventional WPT system except for RX coils and power switches. In the proposed system, one coil of RX is split into two small coils (L_{RX1}, L_{RX2}) that are connected with power switches (S_1, S_2), respectively, as shown in Fig. 3. The reason for using the two coils is that the proposed WPT system simultaneously operates to accumulate of the energy from the primary coil and transfer the previously accumulated energy to the battery. Fig. 4(a) and (b) shows the simplified structures with a series compensation and the operational waveforms of the proposed system, respectively. T_{res} is an interleaved switching period. By turning ON/OFF S_1 and S_2 in an interleaved manner, it is possible to efficiently transfer the energy from the primary to the secondary and from the secondary to the battery in each coil, respectively. While S_1 is switched ON to accumulate the energy from the primary coil by resonating between L_{RX1} and C_{RX1}, S_2 is switched OFF to transfer the energy previously stored in the $L_{RX2}C_{RX2}$ tank to the battery. On the contrary, when S_2 is switched ON to resonate between L_{RX2} and C_{RX2} for multiple cycles, S_1 is switched OFF to transfer the previously

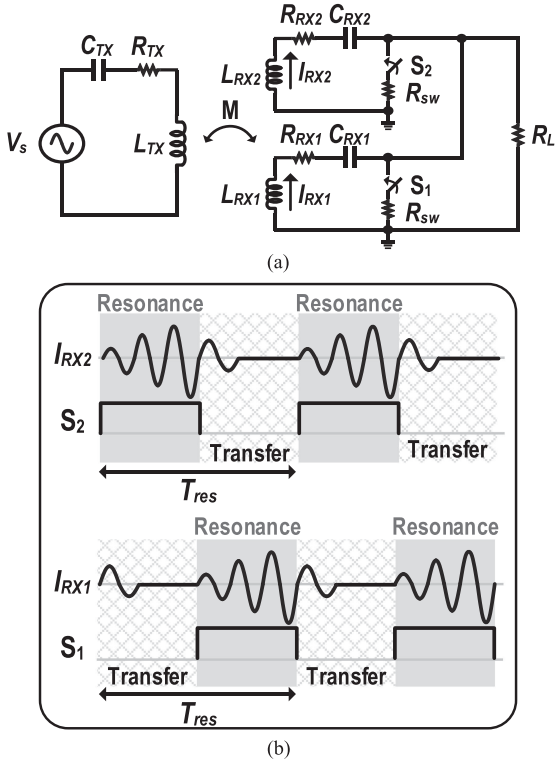

Fig. 4. (a) Simplified structures and (b) operational waveforms of the proposed WPT system.

accumulated energy. Assuming that the parasitic resistance of S_1 or S_2 (R_{SW}) is negligible for a simple analysis, R_L can be modeled as zero at the *LC* resonance. Thus, the power efficiency ($\eta_{1,2,pro}$) delivered from the primary to the secondary in the proposed WPT system is given by

$$\eta_{1,2,\text{pro}} = \frac{R_{\text{refl,pro}}}{R_{\text{TX}} + R_{\text{refl,pro}}} \tag{3}$$

with

$$R_{\text{refl,pro}} = \frac{M^2 \cdot w^2}{R_{\text{RX}}}. \tag{4}$$

Also, the power efficiency ($\eta_{2,L,\text{pro}}$) delivered from the secondary to the RX in the proposed system can be as follows:

$$\eta_{2,L,\text{pro}} = \frac{R_L}{R_{\text{RX}} + R_L}. \tag{5}$$

The merit of using dual coils with the interleaved switching is that $\eta_{1,2,pro}$ from (3) can be isolated with R_L, while $\eta_{2,L,\text{pro}}$ from (5) is defined by R_L, not by equivalent resistance. In other words, high $\eta_{1,2,pro}$ and $\eta_{2,L,\text{pro}}$ can be achieved at the high R_L without modulating the equivalent resistance by controlling the duty cycle in [8] and [10].

Now, we discuss the power loss of S_1 and S_2. As shown in Fig. 4(b), most high current of each RX coil flows while S1 (or S2) turns ON in T_{res}. By adopting the equations in [18], thus the current of each RX coil (I_{RX}) can be defined as follows:

$$I_{\text{RX}}(t) \simeq \left(\frac{V_1}{R_{\text{RX}} + R_{\text{SW}}} \left(1 - e^{-\alpha t}\right) \right) \cdot \sin(wt) \tag{6}$$

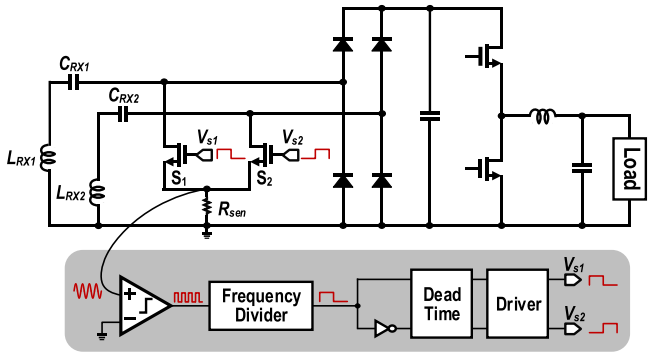

Fig. 5. Circuit implementation of the proposed WPT receiver.

with

$$V_1 = \frac{w \cdot M \cdot V_s}{R_{\mathrm{TX}} + \frac{w^2 M^2}{R_{\mathrm{RX}} + R_{\mathrm{SW}}}}. \tag{7}$$

From (6), the rms current of each RX coil ($I_{\mathrm{RX,rms}}$) is given by

$$I_{\mathrm{RX,rms}} = \sqrt{\frac{1}{T_{\mathrm{res}}} \int_0^{T_{\mathrm{res}}/2} \left(I_{\mathrm{RX}}(t)\right)^2 dt}. \tag{8}$$

Therefore, we can define that the power loss ($P_{\mathrm{loss,sw}}$) of the each switch can be defined as follows:

$$P_{\mathrm{loss,sw}} = I_{\mathrm{RX,rms}}^2 \cdot R_{\mathrm{SW}}. \tag{9}$$

Since $P_{\mathrm{loss,sw}}$ does not exist in the conventional structure, it should be considered to achieve high efficiency in the proposed WPT structure.

If a parallel compensation is used in the RX to adopt the interleaved method, not the dual RX coils but dual RX capacitors should be used. However, since four power switches and a peak voltage detector, which is difficult to implement, should be required for the dual capacitor WPT system, we selected the dual coils WPT system with series compensation to check the effect of the interleaved switching.

Fig. 5 shows the circuit implementation of the proposed WPT receiver. Four diodes (PMEG3050EP) were used for the rectifier, and the buck converter (MPM3620) was used for the output regulation of 5 V. To avoid the hard switching of S_1 and S_2, sensing resistor R_{sen} (KRL1632E) and comparator (LT116) were used to detect the zero current sensing of L_{RX1} and L_{RX2}. By dividing the frequency of the output signal of the comparator with the frequency divider that was implemented as D-type flip flops (M74HCT74), interleaved duty signals (V_{s1}, V_{s2}) were generated to drive S_1 and S_2 (FDMC7692) with a gate driver (UCC27528).

III. Measurement Results

A prototype of the proposed WPT system was verified with an experimental setup, as shown in Fig. 6. We used a 21-turn Litz wire-wound TX coil, of which diameter was 11.5 cm. To compare the performance between the conventional and the proposed structure, we made two types of RX coils: one was a coil made of 7-turn Litz wire (2 μH) for the conven-

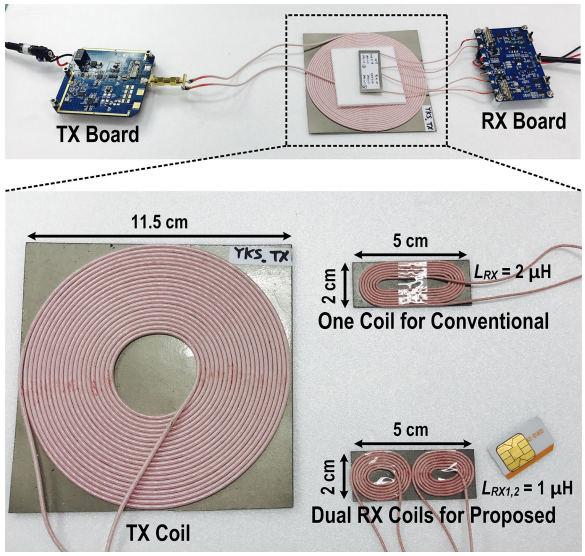

Fig. 6. Experimental setup.

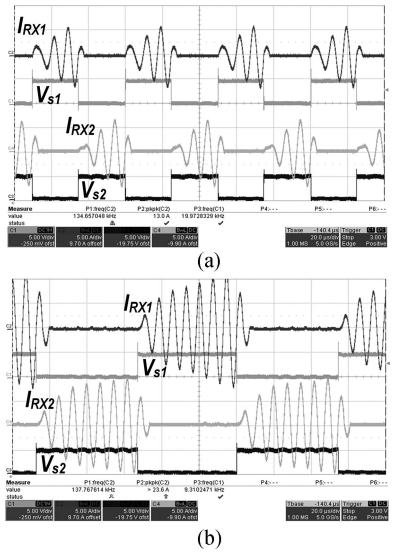

Fig. 7. Measured waveforms. (a) For three duty cycle. (b) For seven duty cycle.

Gear-Fit2 [17]. The other was two coils (each 1 μH) made of 7-turn Litz wire for the proposed structure with the same dimension. We set a fixed operating resonant frequency of the TX and RX as 140 kHz and adjusted it by controlling the value of the compensated capacitors. A precision power supply (Keysight N6705B) was used to provide power for the TX inverter. To measure the performance under various conditions, the charging current drawn from the output voltage of the buck converter was modeled as a system dc electronic load (Agilent 6060B). To check the sensitivity of the RX coil position with respect to the TX coil, a network analyzer (Keysight E5072A) was used to obtain the mutual inductance between the coils. In the center of the TX coil, the highest mutual inductance of 0.93 μH was achieved, while the lowest mutual inductance of 0.122 μH was obtained at the edge of the TX coil.

The measured waveforms of the RX coil current for three duty

TABLE I
PERFORMANCE COMPARISON

	[13]	[14]	[5]	This work	
WPT Application	Mobile	Mobile	Wristband	Wristband	
Frequency	6.78 MHz / 165 kHz	6.78 MHz	200 kHz	140 kHz	
Control Method (# of RX Coils)	Conventional (One Coil)	Conventional (One Coil)	Conventional (One Coil)	Conventional (One Coil)	Interleaving Switching (Two Coils)
RX Coil Size	2.8 × 2.8 cm^2	2.5 × 2.5 cm^2	2.8 × 2.8 cm^2	2 × 5 cm^2	Each 2 × 2.5 cm^2
L_{RX} (Turn)	7.5 μH (N/A)	N/A (N/A)	10 μH (N/A)	2 μH (7)	Each 1 μH (7)
End-to-End Efficiency @ R_L = 100 Ω	< 10 %*	< 10 %*	< 10 %*	9.25 %	15.92 %

*Estimated from measured result graphs

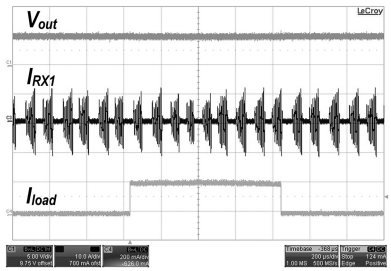

Fig. 8. Measured waveforms in load transition between 10 and 100 Ω.

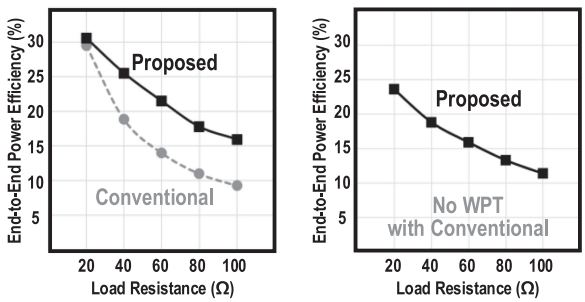

Fig. 9. Measured graphs of end-to-end efficiency as varying output resistance at (a) coil distance = 5 mm and (b) coil distance = 10 mm.

respectively. As the load resistance changed, the duty cycle was manually controlled to achieve high power efficiency [16]. Even the peak-to-peak current of RX coils was over 20 A; we checked that the temperature of RX coils did not go up significantly as less as 45 °C. This is because the current did not continuously flow in each coil by interleaved switching. In addition, the high current of RX coils does not cause a problem to the battery. This is because the high current does not flow directly into the battery, but through the rectifier, the buck converter, and the charger.

To indirectly check the quality of charging of the proposed WPT system, we measured an output voltage of the buck converter (V_{out}) in load transition between 10 and 100 Ω, as shown in Fig. 8. Since V_{out} was constantly regulated in the load transition, it can be said that the charging of the proposed WPT system is not affected by the sudden change of the charging current.

Fig. 9 shows the measured graphs of end-to-end efficiency as varying with the output resistance. The end-to-end efficiency was defined as the output power of the electronic load that was divided by the TX power of the dc power supply. While the efficiency of the conventional system was sharply reduced as the output resistance was increased, and that of the proposed system was somewhat insensitive, even with smaller coils. Thus, when the distance between TX and RX coil was 5 mm, the proposed WPT system achieved higher efficiency of 6.67% at the load resistance of 100 Ω than the conventional WPT system. At the distance of 10 mm, it was possible to transfer the energy from TX to RX by using the proposed system, although it was not possible by using the conventional one.

Table I summarizes the parameter and the performance of the proposed WPT system in comparison with those of previous works for portable device charging. At the high R_L of 100 Ω, those papers achieved low overall efficiency under 10%, because the unwanted energy in TX should be consumed to transfer the energy required to the RX. Although additional two power switches that can endure the flow of high current should be needed to use the interleaved method, the proposed system can achieve over 15% end-to-end efficiency with small RX coils, which could not be attained in previous works. Hence, it is most suitable to the WPT system for wrist wearable devices among the other results reported recently.

IV. CONCLUSION

In this letter, a dual RX coils WPT system with interleaving switching is presented. The proposed system with small RX coils improves the end-to-end efficiency at high R_L by using the RX coils in an interleaved manner. By analyzing and measuring the conventional and proposed structure, the validity of the proposed system was sufficiently verified. Therefore, the proposed WPT system is thought to be the best candidate for wristband wearable devices.

REFERENCES

[1] B.-G. Lee, B.-L. Lee, and W.-Y. Chung, "Wristband-type driver vigilance monitoring system using smartwatch," *IEEE Sens. J.*, vol. 15, no. 10, pp. 5624–5633, Oct. 2015.

[2] J. M. Kang, T. Yoo, and H. C. Kim, "A wrist-worn integrated health monitoring instrument with a tele-reporting device for telemedicine and telecare," *IEEE Trans. Instrum. Meas.*, vol. 55, no. 5, pp. 1655–1661, Oct. 2006.

[3] A. Srivastava, S. V. Vargiya, R. Kumar, and R. Raman, "Medical system based multi-tasking digital wrist watch using VHDL," in *Proc. Int. Conf. Med. Imag., m-Health Emerging Commun. Syst.*, Nov. 2014, pp. 76–79.

[4] Y. M. Roshan and E. J. Park, "Design approach for a wireless power transfer system for wristband wearable devices," *IET Power Electron.*, vol. 10, no. 8, pp. 931–937, Jul. 2017.

[5] S. Wielandt, B. Thoen, J. P. Goemaere, L. De Strycker, and N. Stevens, "Inductive charging of an EDLC powered wristband device for medical measurements," in *Proc. Eur. Conf. Circuit Theory Des.*, Aug. 2015, pp. 1–4.

[6] S. Dumanli, "A wrist wearable dual port dual band stacked patch antenna for wireless information and power transmission," in *Proc. Eur. Conf. Antennas Propag.*, Apr. 2016, pp. 1–5.

[7] S. Jeong *et al.*, "Design and analysis of wireless power transfer system using flexible coil and shielding material on smartwatch strap," in *Proc. IEEE Wireless Power Transf. Conf.*, Jun. 2017, pp. 1–3.

[8] W. X. Zhong and S. Y. R. Hui, "Maximum energy efficiency tracking for wireless power transfer systems," *IEEE Trans. Power Electron.*, vol. 30, no. 7, pp. 4025–4034, Jul. 2015.

[9] Y. H. Sohn, B. H. Choi, E. S. Lee, G. C. Lim, G. H. Cho, and C. T. Rim, "General unified analyses of two-capacitor inductive power transfer systems: Equivalence of current-source ss and sp compensations," *IEEE Trans. Power Electron.*, vol. 30, no. 11, pp. 6030–6045, Nov. 2015.

[10] D. Ahn, S. Kim, J. Moon, and I.-K. Cho, "Wireless power transfer with automatic feedback control of load resistance transformation," *IEEE Trans. Power Electron.*, vol. 31, no. 11, pp. 7876–7886, Nov. 2016.

[11] M. Kiani and M. Ghovanloo, "The circuit theory behind coupled-mode magnetic resonance-based wireless power transmission," *IEEE Trans. Circuits Syst.*, vol. 59, no. 8, pp. 2065–2074, Aug. 2012.

[12] Y.-S. Hwang, S.-C. Wang, F.-C. Yang, and J.-J. Chen, "New compact CMOS Li-ion battery charger using charge-pump technique for portable applications," *IEEE Trans. Circuits Syst.*, vol. 54, no. 4, pp. 705–712, Apr. 2007.

[13] M. Rooij and Y. Zhang, "A 10 W multi-mode capable wireless power amplifier for mobile devices," in *Proc. Int. Exhib. Conf. Power Electron., Intell. Motion, Renew. Energy Energy Manage.*, Jun. 2016, pp. 1–8.

[14] H. Mao, B. Yang, Z. Li, S. Song, and X. Zhao, "Flexible and efficient 6.78 MHz wireless charging for metal-cased mobile devices using controlled resonance power architecture," in *Proc. IEEE Wireless Power Transf. Conf.*, May 2017, pp. 1–4.

[15] S. M. Kim, J. I. Moon, I. K. Cho, J. H. Yoon, W. J. Byun, and H. C. Choi, "Advanced power control scheme in wireless power transmission for human protection from EM field," *IEEE Trans. Microw. Theory Techn.*, vol. 63, no. 3, pp. 847–856, Mar. 2015.

[16] M. Choi, T. Jang, J. Jeong, S. Jeong, D. Blaauw, and D. Sylvester, "A resonant current-mode wireless power receiver and battery charger with −32 dBm sensitivity for implantable systems," *IEEE J. Solid-State Circuits*, vol. 51, no. 12, pp. 2880–2892, Aug. 2016.

[17] Samsung, "Gear Fit2," 2016. [Online]. Available: www.samsung.com/global/galaxy/gear-fit2/

[18] B. Lee *et al.*, "A multicycle Q-modulation for dynamic optimization of inductive links," *IEEE Trans. Ind. Electron.*, vol. 63, no. 8, pp. 5091–5100, Aug. 2016.

[19] S. Barmada and M. Tucci, "Optimization of a magnetically coupled resonators system for power line communication integration," in *Proc. IEEE Wireless Power Transf. Conf.*, Jul. 2015, pp. 1–4.

[20] J. Lim, B. Lee, and M. Ghovanloo, "Optimal design of a resonance-based voltage boosting rectifier for wireless power transmission," *IEEE Trans. Ind. Electron.*, vol. 65, no. 2, pp. 1645–1654, Feb. 2018.

[21] H. S. Gougheri and M. Kiani, "Current-based resonant power delivery with multi-cycle switching for extended-range inductive power transmission," *IEEE Trans. Circuits Syst. I, Reg. Paper*, vol. 63, no. 9, pp. 1543–1552, Sep. 2016.